http://ansinet.com/itj

ITJ

ISSN 1812-5638

INFORMATION TECHNOLOGY JOURNAL

ANSInet
Asian Network for Scientific Information
308 Lasani Town, Sargodha Road, Faisalabad - Pakistan

Information Technology Journal 11 (12): 1744-1750, 2012
ISSN 1812-5638 / DOI: 10.3923/itj.2012.1744.1750

A Quasi Sliding Mode Output Control for Inductively Coupled Power Transfer System

Yue Sun, Xiao Lv, Zhihui Wang and Chunsen Tang
College of Automation, Chong-Qing University, Chong-Qing, China

Abstract: This study presents a quasi sliding mode output control strategy based on feedforward compensation in an improved Inductively Coupled Power Transfer (ICPT) system. In order to reduce the loss of semiconductor switches, a high frequency transformer has been introduced to change the impedance. To increase the efficiency of system, the output voltage is regulated by shifting phase of the gate signals. The quasi sliding mode control function is established by combining feedforward compensation to offset the impact of load disturbance. Computer simulation and practical experiment are conducted to verify the stability and performance of the proposed control system to ensure the control strategy is effective for ICPT systems.

Key words: Inductive coupled power transfer, output control, phase-shift, quasi sliding mode control

INTRODUCTION

Inductively Coupled Power Transfer (ICPT) technology is a practical and flexible technology developed to deliver power wirelessly from the stationary power source to one or more loads. It is becoming increasingly popular in a variety of industrial and commercial applications where high reliability and residue-free operation within exacting or harsh environments may be necessary (Si *et al*., 2008; Boys *et al*., 2007; Wu *et al*., 2011; Villa *et al*., 2012).

Generally, the output of ICPT system is regulated by a DC/DC converter which is located ahead of the inverter. This method is of high cost and low efficiency. For traditional ICPT system, it uses single LC resonant network to maximize the output energy (Tian *et al*., 2012; Wang *et al*., 2004). There is a large current in primary coil which would dramatically increase the losses of inverter and reduce the system efficiency.

At present, there are some difficulties in system controller: nonlinearity, high orders and high frequency. Due to nonlinear switch network in system, switching nonlinearity exists in system dynamic behaviors. At present, in addition to the traditional PID control, robust control (Li *et al*., 2011, 2012; Wang *et al*., 2009) is used in ICPT system but there is certain ripple and it's so difficult in selecting the weighting functions. Because the inverter is just periodic variable structure system, the sliding mode control is a better method with strong adaptability (Zhang and Qiu, 2006; Xu *et al*., 2007; Wan *et al*., 2011; Tang *et al*., 2012; Kang and Jin, 2010; Zribi and Al-Rifai, 2006; Xizheng and Yaonan, 2011; Rabi, 2006; Lasaad *et al*., 2007). However, in order to eliminate the chattering problem in traditional sliding mode control, the common method is the quasi sliding mode control (Slotine and Sastry, 1983). As an improvement of traditional sliding mode control, the quasi sliding mode control doesn't require the control structure switching on switching surface. It can vary the structure on the boundary layer so that continuous feedback control can be occurred within the boundary layer. With these differences it makes the quasi sliding mode control avoid or weaken the chattering fundamentally. Besides, for ICPT system, there are many perturbation actions (such as load disturbance, frequency disturbance (Li *et al*., 2012), so the application of traditional control way is limited.

Based on the above analysis, this study presents quasi sliding mode control strategy with feed forward compensation in improved ICPT system. A high frequency transformer is set up which reduces loss and makes the impedance between inverter and resonant network match. Moreover, a phase-shift method is proposed to realize the rapid regulation of the output voltage.

IMPROVED ICPT SYSTEM

The circuit topology of improved ICPT system is shown in Fig. 1. Similar to the traditional ICPT system, it consists of two independent sections named primary part and secondary part.

In primary part, DC input voltage V_d is selected as energy input. A high frequency transformer network is added between the full bridge inversion networks, made up of S1, S2, S3 and S4 and resonant network comprising resonant inductance L_p and capacitance C_p. In secondary part, energy pickup coil (L_s) receives energy from primary part and produce resonance in network comprising

Corresponding Author: Yue Sun, College of Automation, Chong-Qing University, Chong-Qing, China

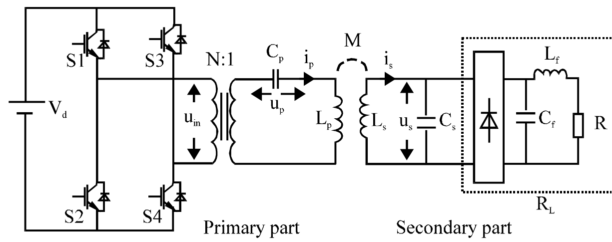

Fig. 1: Improved circuit topology of ICPT system, V_d: DC power supply, S1-S4: Insulating gate bipolar transistor (IGBTs), u_{in}: Output voltage of inverter, N: Winding turns ratio, u_p: Voltage of the primary capacitor C_p, i_p: Current of the primary inductor L_p, M: mutual inductance, i_s: Current of the secondary inductor L_s, u_s: Voltage of the secondary capacitor C_s, Cf: Filter capacitor, L_f: Filter inductor, R: Load resistor, R_L: Equivalent resistance

resonance inductance L_s and capacitance C_s. The rectifier and filter circuits and load can be simplified by an equivalent resistance R_L. The high frequency transformer network not only realizes the electric isolation between the full bridge inverter and resonant network to protect Insulated Gate Bipolar Transistor (IGBT) but also changes the output impedance of inverter to realize the impedance matching of system by changing the winding turns ratio. According to the AC impedance model of system resonant tank, the equivalent impedance Z_s of secondary parts is:

$$Z_s = j\omega L_s + [1/(j\omega C_s)//R_L] \tag{1}$$

where, ω is the operating frequency.

The reflecting impedance Z_r is:

$$Z_r = \omega^2 M^2/Z_s \tag{2}$$

Hence, the system impedance Z_t is:

$$Z_t = N^2\,[Z_r + j\omega L_p + 1/(j\omega C_p)] \tag{3}$$

It can be concluded from Eq. 1-3 that the impedance can be changed by the winding turns ratio N of the high frequency transformer. An appropriate N can be designed to achieve the purpose of the impedance matching.

PHASE-SHIFT REGULATION AND MODELING

One output regulating method which doesn't need additional circuit, economizes the cost and improves the efficiency is to shift the phase of the gate signals. As shown in Fig. 1, the switches S1 and S2, S3 and S4 are complementarily controlled. If both the upper switches S1 and S3 (or both the lower switches S2 and S4) are "on", the AC output voltage from the inverting network is zero. Otherwise, the output voltage will be either positive V_d or negative V_d, depending on the state of the switches. Because of this, phase-shift duty cycle control can be

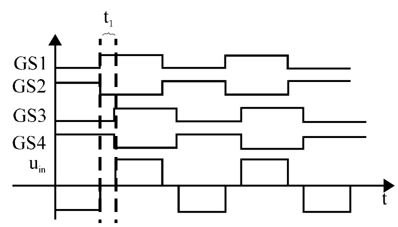

Fig. 2: Phase-shift control, GS1: Gate drive of S1, GS2: Gate drive of S2, GS3: Gate drive of S3, GS4: Gate drive of S4

utilized to regulate the output voltage. Figure 2 shows a situation when the gate signals of S3 and S4 are lagging S1 and S2 by t_1. In this case, the output voltage is a PWM square wave with a duty cycle of $(T-2t_1)/T$. For inverter side, the equivalent impedance of load also is changed.

The relationship between the inverter output voltage u_{in} and phase-shift angle α is:

$$U_{in} = \frac{2\sqrt{2}}{\pi} V_d \cdot \cos\frac{\alpha}{2} \tag{4}$$

where, α is $2\pi t_1/T$.

According to t he Kirchhoff's voltage law and current law, the system can be described as follows (Sun *et al*., 2005):

$$\begin{cases} di_p/dt = L_s\lambda(V_d S(t)/N - u_p - L_p u_s/M) + u_s/M \\ du_p/dt = i_p/C_p \\ di_s/dt = M\lambda(V_d S(t)/N - u_p - L_p u_s/M) \\ du_s/dt = i_s/C_s - u_s/R_L C_s \end{cases} \tag{5}$$

where, λ is $1/(L_p L_s - M^2)$.

$$S(t) = \begin{cases} 1 & t_1 < t \le T/2 \\ 0 & 0 < t \le t_1,\ T/2 < t \le T/2 + t_1 \\ -1 & T/2 + t_1 < t \le T \end{cases}$$

where, i_p, u_p, i_s and u_s represents the exciting current, the voltage of resonant capacitor C_p, the pick-up current and pick-up voltage. The Eq. 5 can be described as:

$$\frac{dx}{dt} = Ax+Bu \tag{6}$$

Where:

$$x = [x_1, x_2, x_3, x_4]^T = [i_p, u_p, i_s, u_s]^T$$

A and B as the constant matrixes denote the system matrix and control matrix.

QUASI SLIDING MODE CONTROLLER DESIGN

From the Eq. 5, the ICPT system is just a variable structure system, so the sliding mode control strategy has strong adaptability for this system. In sliding mode control strategy, the system dynamics is forced by the controller to stay confined in a subset of the state space denominated sliding surface. That is, one first constructs a Lyapunov function and then tries to and a control law to make the derivative of the Lyapunov function negative definite. As the method provides robustness characteristics, there is a major problem, the chattering phenomenon, usually encountered in the practical implementation. This phenomenon is highly undesirable because it may excite the high-frequency unmodeled dynamics.

According to the Eq. 5, the new state space description about errors of each state can be obtained as follows:

$$de/dt = A'e+B'u+F \tag{7}$$

Where:

$$e=[e_1,e_2,e_3,e_4]^T=[i_p-i_{p(ref)},u_p-u_{p(ref)},i_s-i_{s(ref)},u_s-u_{s(ref)}]^T$$

$$A'=\begin{bmatrix} 0 & -L_s\lambda & 0 & (1-L_pL_s\lambda)/M \\ 1/C_p & 0 & 0 & 0 \\ 0 & -M\lambda & 0 & -L_p\lambda \\ 0 & 0 & 1/C_s & -1/(R_LC_s) \end{bmatrix}$$

$$B'=[L_s\lambda/N,0,M\lambda/N,0]^T$$

$$F=[F_a,F_b,F_c,F_d]^T$$

$$F_a=(1-L_pL_s\lambda)u_{sr}/M-L\lambda u_{pr}-\dot{i}_{pr};F_b=i_{pr}/C_p-\dot{u}_{pr}$$

$$F_c=-L_p\lambda u_{sr}-M\lambda u_{pr}-\dot{i}_{sr};F_d=i_{sr}/C_s-u_{sr}/(R_LC_s)-\dot{u}_{sr}$$

$i_{p(ref)}$, $u_{p(ref)}$, $i_{s(ref)}$ and $u_{s(ref)}$ represent the reference values of i_p, u_p, i_s and u_s.

The switching function (sliding surface) s can be described as:

$$s = k_1e_1+k_2e_2+k_3e_3+e_4 \quad (k_1>0, k_2>0, k_3>0) \tag{8}$$

where, k_1, k_2 and k_3 represent the control parameters termed as sliding coefficients.

So, it can be obtained:

$$\dot{s}=k_1\dot{e}_1+k_2\dot{e}_2+k_3\dot{e}_3+\dot{e}_4=a_1e_1+a_2e_2+a_3e_3+a_4e_4+bu+\Gamma \tag{9}$$

Where:

$$a_1=k_2/C_p;a_2=-k_1L_s\lambda-k_3M\lambda;a_3=1/C_s$$
$$a_4=k_1(1-L_pL_s\lambda)/M-k_3L_p\lambda-1/(R_LC_s)$$
$$b=(k_1L_s\lambda+k_3M\lambda)/N;\Gamma=k_1F_a+k_2F_b+k_3F_c+F_d$$

According to the generalized sliding mode conditions $s.\dot{s}<0$, it can be obtained:

$$\begin{cases} u_s^+<(-F-a_1e_1-a_2e_2-a_3e_3-a_4e_4)b^{-1}, s>0 \\ u_s^->(-F-a_1e_1-a_2e_2-a_3e_3-a_4e_4)b^{-1}, s<0 \end{cases} \tag{10}$$

Here, the normal movement segment can be limited with exponential reaching rate to improve its dynamic quality. The exponential reaching rate can be described as:

$$ds/dt = \varepsilon sign(s)-cs \quad (\varepsilon, c>0) \tag{11}$$

Then, the control function can be worked out:

$$u=\begin{bmatrix} -\varepsilon sign(s)-\Gamma-(ck_1+a_1)e_1-(ck_2+a_2)e_2 \\ -(ck_3+a_3)e_3-(c+a_4)e_4 \end{bmatrix}b^{-1} \tag{12}$$

The chattering problem of traditional sliding mode control is caused by the sign(s) of Eq. 12. In order to eliminate the chattering, the saturation function sat(s) is used instead of sign(s):

$$sat(s)=\begin{cases} 1 & s>\Delta \\ k's & |s|\le\Delta \\ -1 & s<-\Delta \end{cases} \quad k'=\frac{1}{\Delta} \tag{13}$$

where, Δ represents the boundary layer. The essence of saturation function is that switching control is used beyond the boundary layer while linear feedback control is used within the boundary layer. In this strategy, the system dynamics is forced by the controller to limit in some Δ neighborhood of ideal sliding mode. The quasi sliding mode doesn't require meeting the condition of existence condition within the boundary layer, so there is no switch on the switching surface and the chattering is essentially eliminated. Besides, the quasi sliding mode control has many advantages, such as fast response, insensitive to parametric variable and external disturbance and excellent steady as well as dynamic response.

Substituting Eq. 13-12 and the quasi sliding control function u_s can be rewritten as:

$$u_s = \begin{bmatrix} -\varepsilon \mathrm{sat}(s) - \Gamma - (ck_1 + a_1)e_1 - (ck_2 + a_2)e_2 \\ -(ck_3 + a_3)e_3 - (c + a_4)e_4 \end{bmatrix} b^{-1} = (-\varepsilon \mathrm{sat}(s) + \varphi) b^{-1} \tag{14}$$

Because the main factor of breakage system steady process is the frequent switching of system load in ICPT system, a load disturbance feedforward compensation controller is introduced to improve the control performance of system. This way could reduce the gain of switching term in the sliding mode controller; improve system dynamic performance by the feedforward compensation of external dynamic disturbance.

The feedforward compensation control function u_c can be expressed as:

$$u_c = d.f \tag{15}$$

where, d is the transfer function, f is the load disturbance.

Combining the quasi sliding mode controller and the feedforward compensation controller, the control system is shown in Fig. 3, the designed control function u is:

$$u = u_s + u_c \tag{16}$$

Actually, the system is disturbed by many uncertain factors which include the uncertain of system matrix and external load disturbance, so the system becomes unsteady. So the system can be described accurately as:

$$de/dt = A'e + B'u + Hf + A_\Delta e \tag{17}$$

Let the switching function ds/dt = 0, so it can be obtained:

$$KA'e + KB'u + KHf + KA_\Delta e = 0 \tag{18}$$

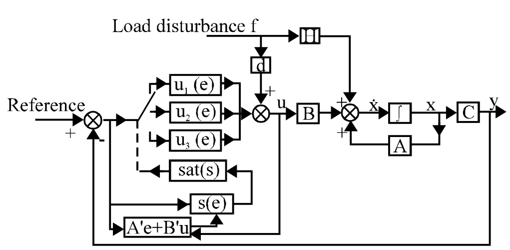

Fig. 3: Block diagram of control system, H: Disturbance matrix, $u_1(e)$~$u_3(e)$: Quasi sliding mode control function, C: Output matrix, y: Output

If the (KB') is nonsingular, the equivalent control function can be described as:

$$u_{eq} = -(KB')^{-1} K (A'e + Hf + A_\Delta e) \tag{19}$$

Substituting Eq. 19-17, it can be obtained the sliding mode motion equation:

$$\begin{aligned} de/dt &= [I - B'(KB')^{-1}K]A'e + \\ &[I - B'(KB')^{-1}K]Hf + [I - B'(KB')^{-1}K]A_\Delta e \end{aligned} \tag{20}$$

According to the Eq. 20, it can be known that if it is satisfied the conditions of:

$$\begin{cases} Hf = B'(KB')^{-1}KHf \\ A_\Delta e = B'(KB')^{-1}KA_\Delta e \end{cases}$$

the sliding mode motion is not influenced by the external load disturbance. So the parameter of the controller should meet the conditions as far as possible. However, we can't eliminate the disturbance completely. In this case, the feedforward compensation is built to counteract the varieties which result from the load disturbance. The condition of the feedforward controller is as follows:

$$d = -\frac{H}{G} \tag{21}$$

where, G stands for the transfer function model of ICPT system.

The block diagram of control system is shown in Fig. 4. The control system consists of the state observer and control function. Based on detecting the output voltage of inverter u_{in} and reference $u_{s(ref)}$, the state observer is used to calculate the real time reference value of $i_{p(ref)}$, $i_{s(ref)}$ and $u_{p(ref)}$. Then the control law is built by the errors of the four states.

When load varies result in the variety of output voltage, the controller can calculate the control output to

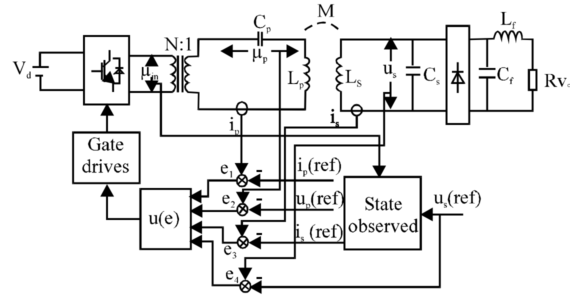

Fig. 4: Structures of ICPT with quasi sliding control, V_o: DC output voltage

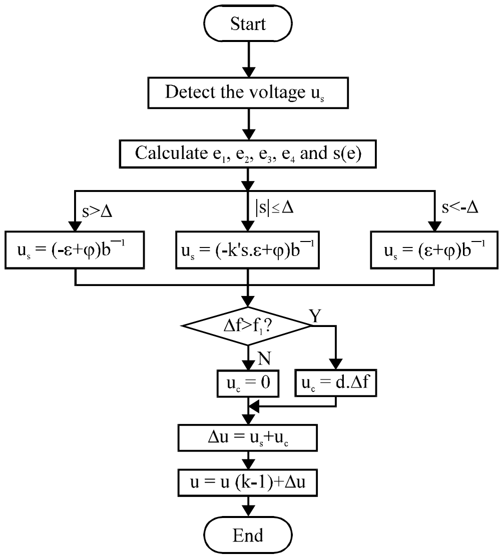

Fig. 5: Control flow chart

keep the output voltage stabilization. The control flow chart is shown in Fig. 5. The voltage u_s of C_s is detected for calculating the switching function. If the sliding mode is out of the boundary layer, the switching control is used, while if the sliding mode is within the boundary layer, linear feedback control is used. However, when the disturbance appears, the feedforward compensation control is used to eliminate the effect of load variation.

SIMULATION AND EXPERIMENT

In order to validate the feasibility of control strategy, the simulation model is built in MATLAB, the parameters are shown in Table 1.

In order to evaluate the performances of the proposed control strategy, the traditional PI control result is compared. The simulation results in load perturbations are shown in Fig. 6. It can be seen that with load resistance changing from 20 to 5 Ω at the instants t = 0.04 sec, the output voltage can faithfully follow the reference input (75 V) with the phase-shift angle gradually decreasing from 61.2-12.6°. However, PI controller takes about 20 msec to adjust the output voltage to reaching the steady state again when load variation occurs. And with a large overshoot about 28 V. It can be seen that about 15 m sec^{-1} is taken to reach the steady state almost without overshoot and oscillation in quasi sliding mode control strategy with feedforward compensation.

$$\alpha = 61.2°, R_L = 20\,\Omega \quad \alpha = 12.6°, R_L = 5\,\Omega$$

In order to verify the simulation results, an ICPT system experiment system is set up as shown in Fig. 4, according to the parameters in Table 1. The experimental results using the quasi sliding mode control strategy with feedforward compensation are shown in Fig. 7.

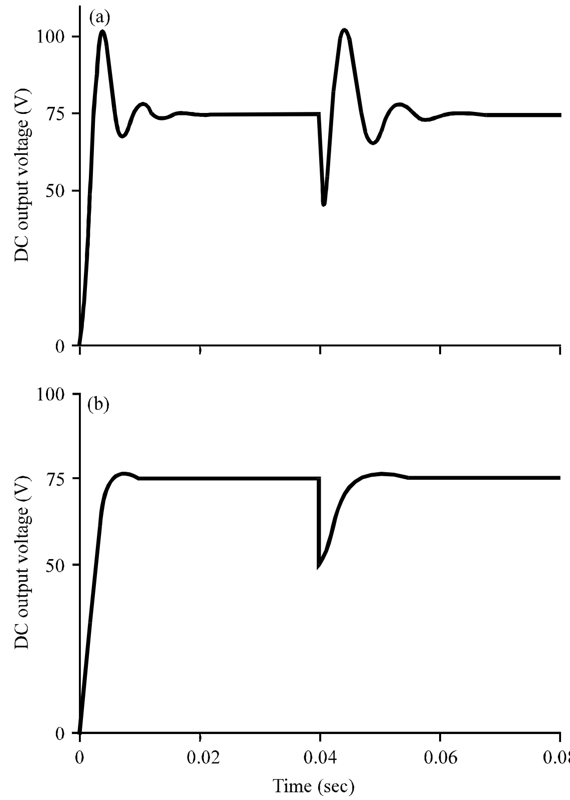

Fig. 6(a-b): Simulation results with different control strategies, (a) PI control and (b) Quasi sliding mode control with feedforward compensation

Table 1: Parameters of ICPT system

Parameters	Values
DC input supply V_d (V)	400.00
Primary resonant inductance L_p (μH)	278.60
Primary resonant capacitance C_p (μF)	0.23
Secondary resonant capacitance L_s (μH)	65.10
Secondary resonant inductance C_s (μF)	0.98
Winding turns ratio N	10.00
Mutual inductance M (μH)	13.50

Figure 7a shows the steady state waveforms including the gate drives signals, input voltage of resonant network and DC output voltage. It can be seen that the DC output voltage is equal to 75 V with the phase-shift angle about 60° when the load resistance is 20 Ω. Due to parasitic parameters in circuit, there exists a certain difference between the experiment and simulation in the phase-shift angle.

From Fig. 7b, it can be known that the dynamic response process just takes 15 m sec^{-1} to successfully achieve tracking the reference value when the load resistance changes from 20-5 Ω. The overshoot and

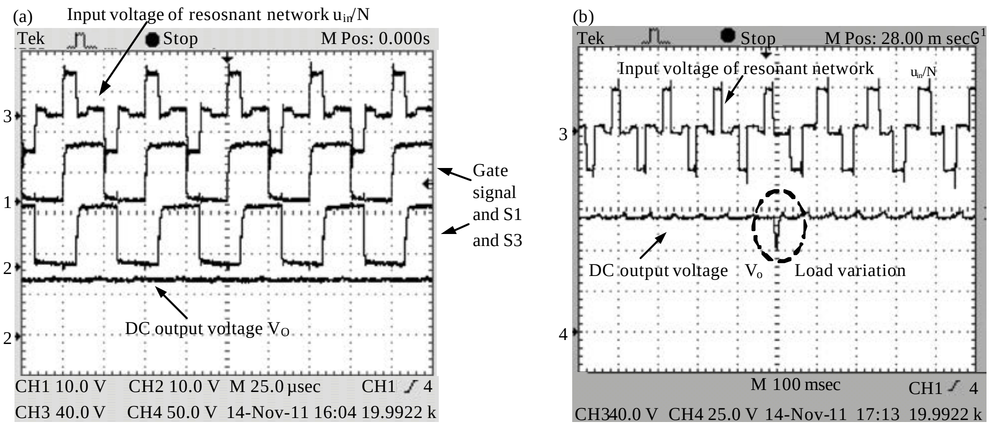

Fig. 7(a-b): The waveforms of the proposed control system, (a) The steady state waveforms of ICPT system and (b) The transient process of proposed control strategy with load variations

oscillation are also weakened in quasi sliding mode control strategy. From these measured waveforms, it is evident that the quasi sliding mode control system has achieved the fast and accurate dynamic tracking performance.

CONCLUSION

This study puts forward an improved ICPT system, which based on the principle of impedance matching. The output is regulated by shifting the phase of the gate signals with the quasi sliding mode control strategy. The feedforward controller is added into the system controller to overcome the voltage fluctuations caused by the variation of load disturbance. The controller is proposed in the paper and its performance is compared with that of a PI controller in order to show the necessary of using such a composite approach by simulation and experiment. The results have verified the feasibility of sliding mode control method on the field of ICPT.

ACKNOWLEDGMENTS

This research work is financially supported by National Natural Science Foundation of China (No. 51007100) and Fundamental Research Funds for the Central Universities (No. CDJXS10170002). Author also would like to give my special thanks to the reviewers of this paper for their contributions to this study.

REFERENCES

Boys, J.T., G.A. Covic and A.W. Green, 2007. Stability and control of inductively coupled power transfer systems. Elect. Power Applic., 147: 37-43.

Kang, P. and Z. Jin, 2010. Neural network sliding mode based current decoupled control for induction motor drive. Inform. Technol. J., 9: 1440-1448.

Lasaad, S., Z. Dalila and A.M. Naceurq, 2007. Adaptative variable structure control for an online tuning direct vector controlled induction motor drives. J. Applied Sci., 7: 3177-3186.

Li, Y.L., Y. Sun and X. Dai, 2011. Mixed-sensitivity H∞ robust control of n-Type Resonant IPT System. J. South China Univ. Technol., 2: 12-19.

Li, Y.L., Y. Sun and X. Dai, 2012. Controller design for an uncertain contactless power transfer system. Informa. Technol. J., 8: 971-979.

Rabi, B.J., 2006. Minimization of harmonics in PWM inverters based on genetic algorithms. J. Applied Sci., 6: 2056-2059.

Si, P., A.P. Hu, S. Malpas and D. Budgett, 2008. A frequency control method for regulating wireless power to implantable devices. IEEE Trans. Biomed. Cir. Syst., 2: 22-29.

Slotine, J.E. and S.S. Sastry, 1983. Tracking control of non-linear systems using sliding surface with application to robotic manipulators. Int. J. Control, 38: 465-492.

Sun, Y., L. Li, X. Dai, Y. Su and Z. Wang, 2005. Discrete mapping modeling and simulation of a full bridge current-fed soft-switching converter. Trans. China Electrotechnical Soc., 20: 23-27.

Tang, R. Q. Zhang and S.J. Wang, 2012. Double adaptive fuzzy sliding mode control scheme for electro-hydraulic velocity servo system. Inform. Technol. J., 11: 620-625.

Tian, Y., Y. Sun, Y. Su, Z. Wang and C. Tang, 2012. Neural network-based constant current control of dynamic wireless power supply system for electric vehicles. Inform. Technol. J., 7: 876-883.

Villa, J.L., J. Salla, J.F.S. Osorio and A. Llombart, 2012. High-Misalignment tolerant compensation topology for ICPT systems. IEEE Trans. Ind. Electron., 59: 945-951.

Wan, Y., C. Hu, D. Wang and L. Wang, 2011. Composite adaptive sliding mode control for electrical servo system using multiple models. Inform. Technol. J., 10: 1673-1682.

Wang, C.S., G.A. Covic and O.H. Stielau, 2004. Power transfer capability and bifurcation phenomena of loosely coupled inductive power transfer systems. IEEE Trans. Ind. Electron., 51: 148-157.

Wang, S.J., N.S. Pai and H.T. Yau, 2009. Robust controller design for synchronization of two chaotic circuits. Inform. Technol. J., 8: 743-749.

Wu, H.H., G.A. Covic, J.T. Boys and D.J. Robertson, 2011. A series-tuned inductive-power-transfer pickup with a controllable AC-voltage output. IEEE Trans. Power Electron., 26: 98-109.

Xizheng, Z. and W. Yaonan, 2011. Adaptive PID-like fuzzy variable structure control for uncertain MIMO systems. Inform. Technol. J., 10: 1793-1800.

Xu, F., H. Ma and X.N. He, 2007. A discrete-time variable rate reaching law controlled current-source inverter. Proc. CSEE, 27: 98-102.

Zhang, L. and S.S. Qiu, 2006. Analysis and experimental study of sliding mode control inverter. Proc. CSEE, 26: 59-63.

Zribi, M. and M. Al-Rifai, 2006. Transient stability of power systems using sliding mode controllers. J. Applied Sci., 6: 580-590.